CGPM 2020

sciforum

Conference Proceedings Paper

Amphiphilic poly(ε-caprolactone) copolyesters of different architectures for drug delivery applications: synthesis, characterization and molecular dynamics

Evi Christodoulou [1,*], Panagiotis A. Klonos [1, 2], Kostas Tsachouridis [1], Maria Notopoulou [1], Alexandra Zamboulis [1], Apostolos Kyritsis [2], Dimitrios N. Bikiaris [1,*]

Published: date
Academic Editor: name

[1] Department of Chemistry, Laboratory of Polymer Chemistry and Technology, Aristotle University of Thessaloniki, GR-541 24, Thessaloniki, Greece; evicius@gmail.com (E.C.), tsaxconofdarkness@gmail.com (K.T.), marynoto@hotmail.com (M.N.), azamboulis@gmail.com (A.Z.), dbic@chem.auth.gr (D.N.B)
[2] Department of Physics, National Technical University of Athens (NTUA), Zografou Campus, 15780, Athens, Greece; pklonos@central.ntua.gr (P.A.K.), akyrits@central.ntua.gr (A.K.)
* Correspondence: evicius@gmail.com (E.C.), dbic@chem.auth.gr (D.N.B); Tel.: +30-2310-997812

Abstract: In the present work, we initially synthesized and for the first time comparatively studied the properties of three amphiphilic copolymers based on PCL, differing in architecture, namely, two star-like copolyesters with 3 and 4 PCL arms based on glycerol and pentaerythritol as multifunctional cores/initiators, respectively, as well as a linear block copolymer based on PCL and methoxy-poly(ethylene glycol) (mPEG). Neat PCL and all copolymers were prepared *in situ* via the ROP of ε-CL and characterized by a combination of techniques (^{1}HNMR/ FT-IR spectroscopy, X-ray diffraction, calorimetry, polarized optical microscopy and broadband dielectric spectroscopy). Focus has been given to the impact of copolymer structure on the crystallization, melting and glass transition and hydration of PCL. The overall recordings indicated that the different polymer architecture results in severe changes in the semicrystalline morphology, which demonstrates the potential for tuning the final product performance (permeability, mechanical). Due to their biocompatibility and low toxicity, these systems are envisaged for use in drug delivery and tissue engineering applications.

Keywords: poly(ε-caprolactone); copolymers; star-like copolyesters; polymer crystallization; molecular dynamics; calorimetry; dielectric spectroscopy.

1. Introduction

Bio-based and biodegradable aliphatic polyesters [1], such as poly(L-lactide) [2], poly(ε-caprolactone) [3], poly(alkylene succinate)s, polyglycerol hyperbranched polyesters [4] etc. serve as excellent "green" candidates for a broad range of applications (biomedical, pharmaceutical, agricultural and industrial), combining biocompatibility, renewability and generally good performance. Further improvement of their properties (mechanical performance, biodegradation rate) can be achieved by copolymerization with a variety of bio-based monomers [5],[6] or by the introduction of reinforcing materials [7]–[9]. Especially when it comes to drug delivery applications, where the release rate is severely affected by several parameters, including the glass transition,

melting point and crystallinity of the employed polyesters, it is crucial to study and potentially tune all these properties [10],[11].

Poly(ε-caprolactone), PCL, the polymer of interest here, is a hydrophobic, non-toxic, biodegradable and biocompatible aliphatic polyester displaying slow *in vivo* hydrolysis in addition to quite high crystalline fractions [12],[13]. It also exhibits a unique compatibilizing ability with various polymers of different types, which most often results in new, modified and enhanced material properties. The known methods for the synthesis of PCL are the enzymatic or radical polymerization and the anionic, cationic or coordinated ring-opening polymerization (ROP) of ε-caprolactone (CL) (**Scheme 1**, in the following). Several studies on PCL have focused on properties related with envisaged chemical and biomedical applications (tissue engineering, scaffolding, drug delivery).

Polymer crystallization is in general assessed by widely known experimental techniques, namely calorimetry [14],[15] and X-ray diffraction [16],[17]. Any modifications in crystallinity, owing to the polymer architecture [18] and/or any filler introduction [19], impose direct impacts on the chains diffusion of the amorphous bulk-like polymer (mobile amorphous fraction, MAF). The latter are reflected on the glass transition and segmental molecular dynamics.

In the present work, the three PCL-based copolymers prepared by original synthetic strategies, are studied and reported here along the lines of future applications in the fields of tissue engineering and drug delivery. For this investigation, we employed X-ray diffraction (XRD), polarized optical microscopy (POM), nuclear magnetic resonance (^{1}H NMR), Fourier-transform infrared (FTIR) spectroscopy, differential scanning calorimetry (DSC), and isothermal water sorption in equilibrium, to study the impact of copolymer structure on the crystallization, melting and glass transition and hydration of PCL. Finally, to investigate the molecular dynamics of the local and the segmental type, we employed the advanced technique of broadband dielectric spectroscopy (BDS), characterized by quite high resolving power. The dielectric-calorimetric map for these copolymers is shown here for the first time, to the best of our knowledge.

2. Experiments

The bulk polymerization of ε-CL was carried out in a round-bottom flask equipped with a mechanical stirrer in a high vacuum apparatus. The catalyst THE ($Sn(Oct)_2$) was added as a solution in toluene at a final concentration of 1×10^{-4} mole per mole of the monomer. The polymerization mixture was de-gassed and purged with nitrogen three times. The ROP reaction (**Scheme 1**) was carried out for 3 h at 190 °C, followed by an increase of the reaction temperature from 210 to 240 °C over a period of 90 min. The non-reacted monomers were removed through distillation by slowly applying high vacuum, to avoid excessive foaming, over a time period of 15 min. Polymerization was terminated by rapid cooling to room temperature (RT).

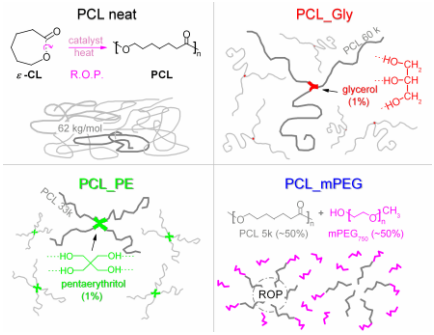

Scheme 1. Schematic view of the materials under investigation, based on PCL prepared by ring opening polymerization (ROP), indicated being the estimated Mw of PCL in each case.

Similarly, the 'PCL_mPEG' copolymer (Scheme 1, Table 1) was synthesized via ROP of ε-CL, using mPEG as the macro-initiator and TEH as catalyst (mPEG/PCL in 1:1 molar ratio). The reaction

mixture was agitated at 150 °C for 1 h in nitrogen (N_2) atmosphere and under constant stirring to ensure that the alcohol was completely dissolved in CL. Then, the catalyst was added to the homogenous reaction mixture and the polymerization proceeded at 160 °C for 6 h under increased stirring and high vacuum. A similar procedure was also followed for the synthesis of the two star-shaped copolymers, 'PCL_Gly' and 'PCL_PE'. The amount of glycerol/pentaerythritol added to the reaction, was fixed to 1 % w/w of ε-CL.

3. Results & Discussion

3.1. Structural characterization

The ^{1}H NMR spectra and the corresponding peak assignments of the prepared copolymers are presented in **Figure 1a**. In the ^{1}H NMR spectrum of neat PCL, the protons near the oxygen atoms [(6) in the insets to **Figure 1a**] are the most de-shielded, and they appear at 4.03 ppm, followed by the protons near the carbonyl group at 2.27 ppm.

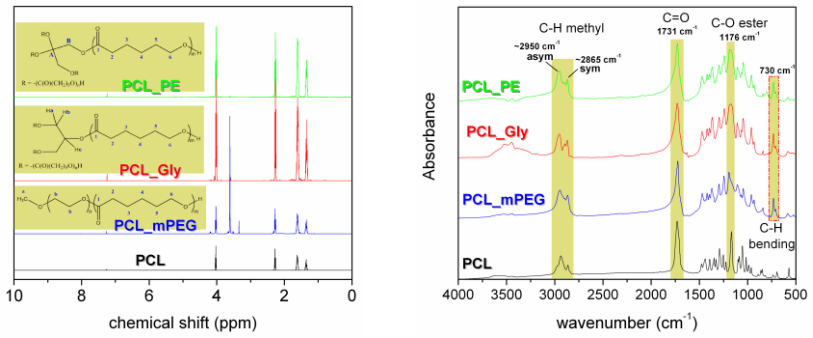

(a) (b)

Figure 1. (a) 1H NMR spectra of PCL and the three prepared copolyesters (insets), and (b) FTIR spectra of neat PCL and the three prepared co-polyesters. Included on the plot are the molecular origins of the marked areas.

The protons (3) and (5) appear at 1.61 ppm, while the peak at 1.36 ppm corresponds to the most shielded methylene protons of the chain (4). The spectra of the synthesized materials present all the aforementioned characteristic peaks of PCL. The PCL_mPEG copolymer also exhibits two new clearly visible peaks, one at 3.61 ppm attributed to the methylene protons (b), and one at 3.34 ppm due to the methyl protons (a) of the end $-OCH_3$ group of mPEG. For PCL_Gly and PCL_PE, due to the low amount of glycerol/pentaerythritol used during synthesis, their protons are hard to distinguish in the ^{1}H NMR spectra. According to literature on glycerol esters [20], its protons appear at 4-5 ppm. Consequently, the small peaks at 4.12, 4.27 and 5.23 ppm in PCL_Gly spectrum could be attributed to the two equivalent Ha, Hb and to the Hc proton, respectively. Similarly, the peak at 4.08 ppm in the spectrum of PCL_PE is assigned to the B protons of pentaerythritol unit.

In addition to ^{1}H NMR, FTIR spectroscopy was also employed to confirm the structure of the synthesized materials. All recorded infrared spectra are shown in the comparative **Figure 1b**, the results verifying the successful synthesis of the copolyesters. More specifically, the main characteristic peaks of PCL are clearly distinguished; C_{sp^3}–H stretching is at the origins of the peaks located at 2950 cm^{-1} and 2865 cm^{-1}, asymmetric and symmetric, respectively, whereas the stretching vibration of the C=O carbonyl group and the C–O ester group appear at 1731 cm^{-1} and 1175 cm^{-1}, respectively. These findings are in accordance with previous work on caprolactone [13]. As in the ^{1}H NMR studies, there are no major peaks associated with the added alcohols (1 %), presumably due to the similar characteristic groups and the overlapping of the polymer-related peaks with those of the alcohols. However, upon detailed examination, we can observe the increased intensity of C–H stretching absorbance peaks, as well as the appearance of a new peak at 730 cm^{-1} (dash-dotted area

in **Figure 1b**) assigned to the C–H bending vibration, potentially owing to the addition of the extra methylene groups on the polymer chain.

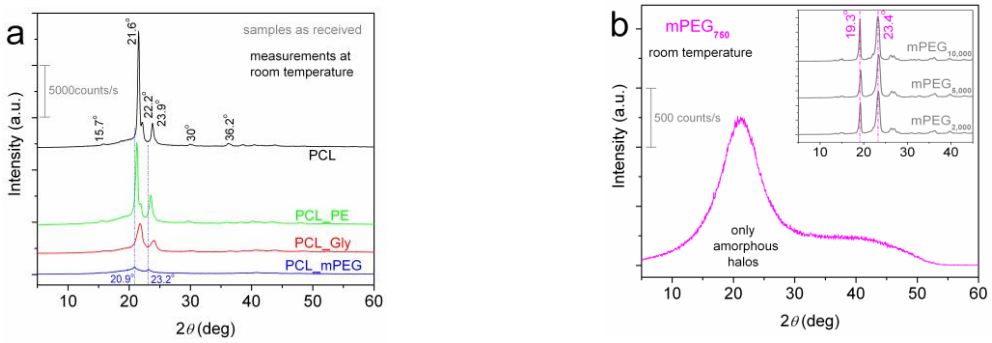

Figure 2. (a) XRD spectra shown comparatively for all samples as received at room temperature (RT~25 °C). Indicated are the main crystalline diffraction peaks and the corresponding 2θ positions. (b) Shows the XRD data for neat mPEG750, exhibiting amorphous behavior at RT.

XRD measurements in **Figure 2** correspond to initially prepared samples that have stayed at RT. All PCL-based samples exhibit a semicrystalline view in XRD in **Figure 2a**. Neat PCL demonstrates mainly 3 crystalline peaks in XRD, i.e. at the 2θ positions of 21.6°, 22.2° and 23.9°. PCL_Gly and PCL_PE demonstrate qualitatively similar XRD spectra with neat PCL. On the other hand, PCL_mPEG shows quite weak crystalline peaks, moreover, at lower 2θ positions in **Figure 2a**. As we will discuss in a following section (DSC), this is due to the lower and quite more wide melting temperature range of PCL_mPEG (–20 to 45 °C). Thus, the data shown in **Figure 2a** for PCL_mPEG at RT, correspond to a partly melted sample. In support to that, neat mPEG750 shows an amorphous XRD spectrum in **Figure 2b**, as its melting occurs at temperatures quite below RT. In the inset to **Figure 2b** we have included results by XRD for mPEG750 samples of larger M_w (2k, 5k and 10k) that are semicrystalline at RT and exhibit 2 main crystalline peaks at the 2θ of 19.3° and 23.4°.

3.2. Crystallization and glass transition

The thermal transitions of the polymers were assessed by DSC of the conventional mode. The respective results are shown in **Figure 3**, while the values of main interest are listed in **Table 1**. In the order of increasing temperature, all samples exhibit a glass transition step in the range from –74 to –66 °C, crystallization between 10 and 35 °C and melting of crystals between 20 and 65 °C.

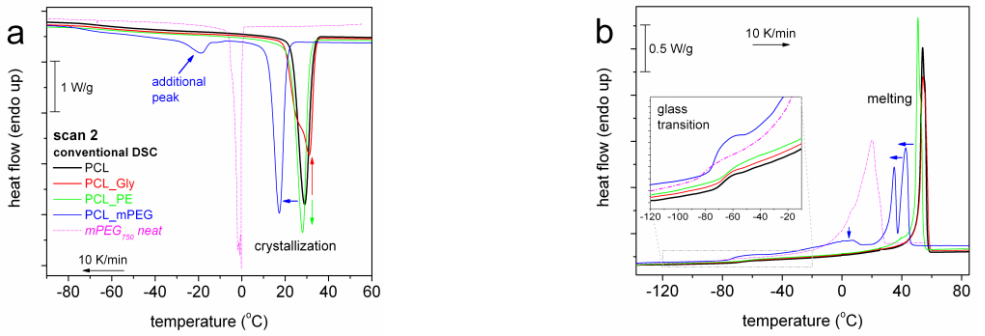

Figure 3. DSC thermograms of scan 2 for all samples studied, during (a) cooling from melt and (b) subsequent heating. The heat flow values are normalized to the sample mass.

Initial PCL crystallizes at 29 °C and melts at 54 °C (**Table 1**) producing a CF of 0.47 wt. It is clear already from a glance at the raw data of **Figure 3**, that PCL_Gly and PCL_PE exhibit crystallization/melting similar to PCL, with PCL_PE crystallizing/melting at slightly lower temperatures and showing slightly higher CF = 0.51 wt whereas PCL_Gly crystallizing/melting at slightly elevated temperatures and showing slightly higher CF = 0.47 wt. Interestingly, PCL-mPEG

demonstrates quite different crystallization and melting characteristics as compared to initial PCL and the rest of the copolymers. First, this sample exhibits additional crystallization and melting peaks, whereas it crystallizes in general at lower temperatures (–19 and 17 °C) and, also, melts at lower temperatures (12 and 64 °C). T_c decreases in the order of samples PCL → PCL_Gly → PCL_PE → PCL_mPEG. This order is almost the same with that of decreasing M_w. Thus, apart from the copolymer structure, it seems that the PCL chain/arm length affects both the crystals nucleation and the lamellar packing (density).

Table 1. Values of interest by DSC measurements of scan 2: crystallization and melting temperatures/enthalpies, (T_c, ΔH_c) and (T_m, ΔH_m), crystalline fraction, CF, glass transition temperature, Tg and heat capacity change during glass transition, Δc_p.

sample	M_w[a] (g/mol)	w_{PCL} (wt%)	conventional DSC – scan 2						
			T_c (°C)	ΔH_c (J/g) (±1)	CF (wt)	T_g (°C)	Δc_p (J/gK) (±0.02)	T_m (°C)	ΔH_m (J/g) (±3)
PCL	62k	100	29	66	0.47	–70	0.13	54	75
PCL_ Gly	60k	99	31	65	0.47	–68	0.13	54	71
PCL_ PE	33k	99	28	70	0.51	–66	0.14	51	75
PCL_ mPEG	5k	48	17(–19)[b]	58(8)[b]	0.87(0.08)[b]	–73	0.33	35/43(0)[b]	64(12)[b]
$mPEG_{750}$	750	100	0	103	0.52	–83	0.14	20	110

[a] Estimated by Gel permeation chromatography (GPC).

[b] Multiple and well separated crystallization and melting events, probably of mPEG750 (low temperatures) and PCL (higher temperatures).

These results by DSC scan 2 are compatible with findings by POM during hot crystallization (from the melt) at 40 °C in **Figure 4**. Therein, comparing between the two star-like copolyesters, PCL_Gly consists of large crystals (higher T_c/T_m) that do not fill the polymer volume, whereas PC_PE exhibits also smaller crystals (lower T_c/T_m) filling more efficiently the polymer volume. It is worth to recall the different structure of these materials (3 and 4 –arms stars) of shorter arm lengths as compared to neat PCL, which should play crucial role on both the nucleation and the growth of crystals. Practically, the star-like copolyesters demonstrated more large crystallites as compared to neat PCL.

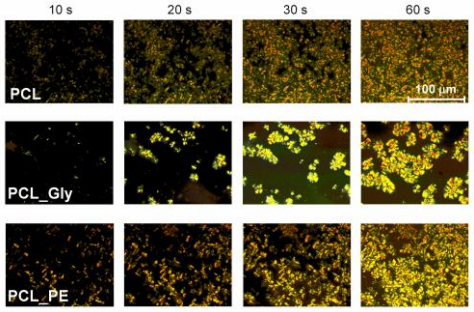

Figure 4. POM micrographs for (top) neat PCL, (middle) PCL_Gly and (bottom) PCL_PE, initially melted, during isothermal crystallization at 40 °C, at the time steps of 10, 20, 30 and 60 seconds.

3.3. Molecular dynamics

The raw BDS results can be seen in **Figures 5**,**6**, in the form of isothermal curves of the imaginary part of dielectric permittivity, ε'', against frequency, f. The dielectric investigation involves measurements both above the T_g, to assess the dynamics related to the glass transition, i.e. the so called main α relaxation of the polymer, as well as measurements at very low temperatures (below T_g) to record effects of local molecular motions. Indeed, in **Figure 5** we observe in the form of peaks of ε'' three discrete types of dynamics. At $T<T_g$, we record the two secondary-local relaxations γ and β of PCL [21]. At $T>T_g$, it is expected the entrance of the α relaxation into the frequency window, however, it is not clearly visible in most of the samples (**Figures 5a-c**), most probably because it is exceptionally weak.

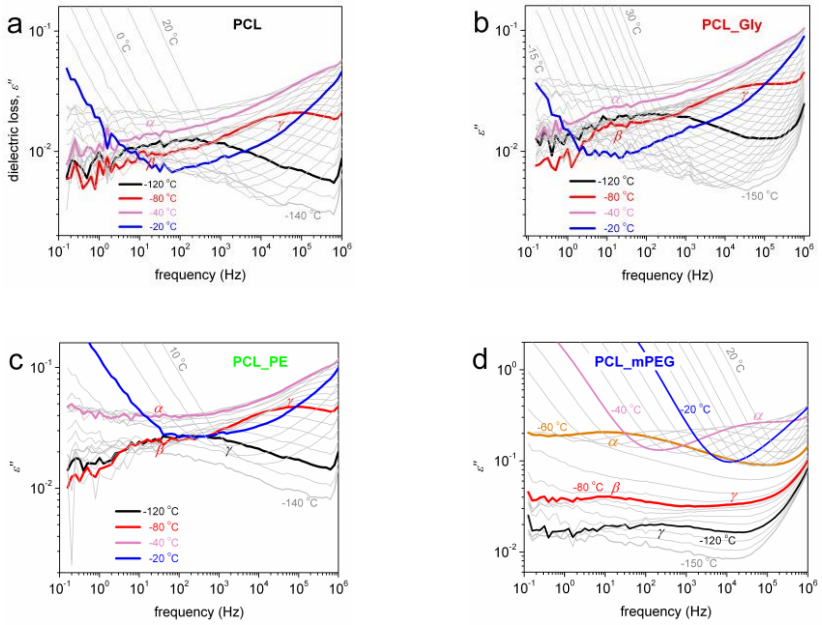

Figure 5. BDS raw data in terms of the frequency dependence of the imaginary part of dielectric permittivity, ε'', for (a) pure PCL and the corresponding copolymers (b) PCL_Gly, (c) PCL_PE, and (d) PCL_mPEG. The recorded relaxation processes (α, β, γ) are indicated on the plots at selected temperatures.

Interestingly in **Figures 5d**,**6b**, α relaxation in PCL_mPEG is observed by bare eye, for example at –60 °C with its peak located between 10^1 and 10^2 Hz (**Figure 5d**) and at –40 °C (**Figure 6b**) between 10^4 and 10^5 Hz. Considering that α relaxation is the dielectric analogue of the glass transition, the latter results come in agreement with the 'glass transition' strength in DSC (Δc_p, **Table 1**). Thus, this is the case of α relaxation of mPEG.

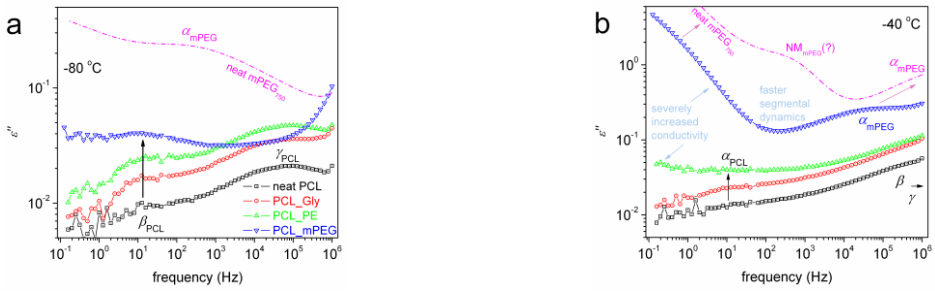

Figure 6. (a,b) Comparative isothermal plots of ε''(f) at (a) –80 oC and (b) –40 oC for all samples. Indicated are the recorded relaxation peaks (γ, β, α).

4. Conclusions

In this article, we synthesized a series of PCL based copolyesters of different architectures, namely, two consisting of 3- and 4-'PCL arms' star-like copolymers, and a linear block copolymer of PCL:mPEG at the molecular ratio of 1:1. Next to the successful synthesis (^{1}H NMR, FTIR), based on the overall results of the employed techniques (DSC, XRD, POM, BDS) it was found that CF of PCL increases in the copolymers in the order PCL ~ PCL_Gly > PCL_PE >> PCL_mPEG, whereas at the same order the T_c decreases, coinciding with the corresponding drop of M_w. The results revealed retarded nucleation in the copolymers along with changes in semicrystalline morphology. With the exception of PCL_mPEG, the single glass transition step recorded arises from PCL with CF~50 wt%, and is slightly elevated as a result of the star-like architecture. The situation in PCL_mPEG was found more complex, as the major of amount of PCL was found to crystallize (CF~90 wt%) and, thus, exhibits no glass transition, whereas the majority of $mPEG_{750}$ was found severely amorphous (only 8 wt% in CF) demonstrating a strong segmental mobility. BDS was employed to study the local (β and γ) and the segmental dynamics (α, related to the T_g). These results provide strong support for the main amorphous character of mPEG in the form of copolyester and the highly crystalline character of PCL, along with indications for the formation of core/shell -like structures consisting of small PCL crystallites surrounded by amorphous mPEG segments. Overall, these recordings indicated that the different polymer architecture results in severe changes in the semicrystalline morphology, which demonstrates the potential for tuning the final product performance.

Acknowledgments: The authors wish to acknowledge co-funding of this research by European Union-European Regional Development Fund and Greek Ministry of Education, Research and Religions/EYDE-ETAK through program EPANEK 2014-2020/Action "EREVNO-DIMIOURGO-KAINOTOMO" (project T1EΔK-01612).

Author Contributions: E.C. and D.N.B conceived and designed the experiments; E.C., K.T., M.N., A.Z. and P.A.K performed the experiments; E.C. and P.A.K. analyzed the data; E.C. and P.A.K. wrote the paper, D.N.B. and A.K. supervised the experimental procedure, reviewed and edited the manuscript.

Conflicts of Interest: The authors declare no conflict of interest.

References

[1] Fakirov, S. *Biodegradable Polyesters*; John Wiley & Sons, 2015.

[2] Armentano, I.; Bitinis, N.; Fortunati, E.; Mattioli, S.; Rescignano, N.; Verdejo, R.; López-Manchado, M. A.; Kenny, J. M. Multifunctional Nanostructured PLA Materials for Packaging and Tissue Engineering. *Prog. Polym. Sci.* **2013**, *38* (10–11), 1720–1747.

[3] Ikada, Y.; Tsuji, H. Biodegradable Polyesters for Medical and Ecological Applications. *Macromol. Rapid Commun.* **2000**, *21* (3), 117–132.

[4] Zamboulis, A.; Nakiou, E. A.; Christodoulou, E.; Bikiaris, D. N.; Kontonasaki, E.; Liverani, L.; Boccaccini, A. R. Polyglycerol Hyperbranched Polyesters: Synthesis, Properties and Pharmaceutical and Biomedical Applications. *Int. J. Mol. Sci.* **2019**, *20* (24), 6210.

[5] Safari, M.; Mugica, A.; Zubitur, M.; Martínez de Ilarduya, A.; Muñoz-Guerra, S.; Müller, A. J. Controlling the Isothermal Crystallization of Isodimorphic PBS-Ran-PCL Random Copolymers by Varying Composition and Supercooling. *Polymers (Basel).* **2020**, *12* (1), 17.

[6] Rizis, G.; van de Ven, T. G. M.; Eisenberg, A. Crystallinity-Driven Morphological Ripening Processes for Poly (Ethylene Oxide)-Block-Polycaprolactone Micelles in Water. *Soft Matter* **2014**, *10* (16), 2825–2835.

[7] Raquez, J.-M.; Habibi, Y.; Murariu, M.; Dubois, P. Polylactide (PLA)-Based Nanocomposites. *Prog. Polym. Sci.* **2013**, *38* (10–11), 1504–1542.

[8] Marras, S. I.; Kladi, K. P.; Tsivintzelis, I.; Zuburtikudis, I.; Panayiotou, C. Biodegradable Polymer Nanocomposites: The Role of Nanoclays on the Thermomechanical Characteristics and the Electrospun

Fibrous Structure. *Acta Biomater.* **2008**, *4* (3), 756–765.

[9] Gumede, T. P.; Luyt, A. S.; Muller, A. J. Review on PCL, PBS, and PCL/PBS Blends Containing Carbon Nanotubes. **2018**.

[10] Karavelidis, V.; Giliopoulos, D.; Karavas, E.; Bikiaris, D. Nanoencapsulation of a Water Soluble Drug in Biocompatible Polyesters. Effect of Polyesters Melting Point and Glass Transition Temperature on Drug Release Behavior. *Eur. J. Pharm. Sci.* **2010**, *41* (5), 636–643. https://doi.org/10.1016/j.ejps.2010.09.004.

[11] Karavelidis, V.; Karavas, E.; Giliopoulos, D.; Papadimitriou, S.; Bikiaris, D. Evaluating the Effects of Crystallinity in New Biocompatible Polyester Nanocarriers on Drug Release Behavior. *Int. J. Nanomedicine* **2011**, *6*, 3021–3032. https://doi.org/10.2147/IJN.S26016.

[12] Nanaki, S. G.; Papageorgiou, G. Z.; Bikiaris, D. N. Crystallization of Novel Poly (ϵ-Caprolactone)-Block-Poly (Propylene Adipate) Copolymers. *J. Therm. Anal. Calorim.* **2012**, *108* (2), 633–645.

[13] Terzopoulou, Z.; Bikiaris, D. N.; Triantafyllidis, K. S.; Potsi, G.; Gournis, D.; Papageorgiou, G. Z.; Rudolf, P. Mechanical, Thermal and Decomposition Behavior of Poly (ε-Caprolactone) Nanocomposites with Clay-Supported Carbon Nanotube Hybrids. *Thermochim. Acta* **2016**, *642*, 67–80.

[14] Vega, J. F.; Fernández-Alcázar, J.; López, J. V; Michell, R. M.; Pérez-Camargo, R. A.; Ruelle, B.; Martínez-Salazar, J.; Arnal, M. L.; Dubois, P.; Müller, A. J. Competition between Supernucleation and Plasticization in the Crystallization and Rheological Behavior of PCL/CNT-based Nanocomposites and Nanohybrids. *J. Polym. Sci. Part B Polym. Phys.* **2017**, *55* (17), 1310–1325.

[15] Klonos, P. A.; Tegopoulos, S. N.; Koutsiara, C. S.; Kontou, E.; Pissis, P.; Kyritsis, A. Effects of CNTs on Thermal Transitions, Thermal Diffusivity and Electrical Conductivity in Nanocomposites: Comparison between an Amorphous and a Semicrystalline Polymer Matrix. *Soft Matter* **2019**, *15* (8), 1813–1824.

[16] Wurm, A.; Soliman, R.; Schick, C. Early Stages of Polymer Crystallization—a Dielectric Study. *Polymer (Guildf).* **2003**, *44* (24), 7467–7476.

[17] Wurm, A.; Soliman, R.; Goossens, J. G. P.; Bras, W.; Schick, C. Evidence of Pre-Crystalline-Order in Super-Cooled Polymer Melts Revealed from Simultaneous Dielectric Spectroscopy and SAXS. *J. Non. Cryst. Solids* **2005**, *351* (33–36), 2773–2779.

[18] Papageorgiou, G. Z.; Tsanaktsis, V.; Bikiaris, D. N. Crystallization of Poly (Butylene-2, 6-Naphthalate-Co-Butylene Adipate) Copolymers: Regulating Crystal Modification of the Polymorphic Parent Homopolymers and Biodegradation. *CrystEngComm* **2014**, *16* (34), 7963–7978.

[19] Zhuravlev, E.; Wurm, A.; Pötschke, P.; Androsch, R.; Schmelzer, J. W. P.; Schick, C. Kinetics of Nucleation and Crystallization of Poly (ε-Caprolactone)–Multiwalled Carbon Nanotube Composites. *Eur. Polym. J.* **2014**, *52*, 1–11.

[20] Jiang, G.; Walker, G. S.; Jones, I. A.; Rudd, C. D. Mechanistic Study of Boron Trifluoride Catalyzed E-caprolactone Polymerization in the Presence of Glycerol. *J. Appl. Polym. Sci.* **2006**, *102* (4), 3900–3906.

[21] Koutsoumpis, S.; Poulakis, A.; Klonos, P.; Kripotou, S.; Tsanaktsis, V.; Bikiaris, D. N.; Kyritsis, A.; Pissis, P. Structure, Thermal Transitions and Polymer Dynamics in Nanocomposites Based on Poly (ε-Caprolactone) and Nano-Inclusions of 1-3D Geometry. *Thermochim. Acta* **2018**, *666*, 229–240.